

Modeling, Control and Experiment of a Feedback Active Noise Control System for Free Sound Fields

Shuichi Adachi and Hisashi Sano

Key words : active noise control, acoustics, physical modeling, system identification,

\mathcal{H}_∞ control, automobile

Shuichi Adachi is with the Department of Electrical and Electronic Engineering, Utsunomiya University, 7-1-2 Yoto, Utsunomiya, Tochigi, 321-8585 Japan, E-mail:adachis@cc.utsunomiya-u.ac.jp

Abstract

Feedback active noise control (FB-ANC) systems need no reference signal sensors and their implementation cost is therefore attractive due to the relatively simple configuration. This paper reports the design of an FB-ANC system for free sound fields by \mathcal{H}_∞ control theory based on a lower-order infinite impulse response (IIR) model of the acoustic plant. The acoustic plant, which is an acoustic transmission system from a loudspeaker (i.e. the actuator) to an error microphone (i.e. the sensor), is first devised by using the physical modeling method in conjunction with a system identification result. The feedback controller is next designed to attenuate the noise level in the vicinity of the error sensor by reducing the sensitivity function over the frequency range of interest. \mathcal{H}_∞ control theory is applied to achieve the control objective, because it can formulate the control specifications in terms of the frequency weighting functions in the frequency domain. Finally, the effectiveness of the proposed design procedure is demonstrated by experimental tests.

I. INTRODUCTION

Many studies have been reported on active noise control (ANC) systems, especially feed-forward ANC (FF-ANC) systems⁽¹⁾⁽²⁾. Figure 1 shows a single-input, single-output, and single-error (SISOSE) system, where H and P are respectively the transfer functions from the noise source to the error sensor (microphone), and from the secondary source (loudspeaker) to the error sensor. C represents the transfer function of the feed-forward controller⁽³⁾. The control objective of the ANC system is to reduce the noise level in the vicinity of the error microphone over the frequency range of interest. To achieve this objective, the feed-forward controller calculates the control signal based on the reference and error signals. The best-known FF-ANC system is based on the filtered-x least mean square (LMS) algorithm which has been proposed for adaptive filtering⁽⁴⁾.

One of the problems restricting industrial applications of the FF-ANC system is its high cost, for example, numerous reference signal sensors, i.e. input signals, are required when an FF-ANC system is employed for reducing road noise in the cabin of an automobile⁽⁵⁾⁽⁶⁾, because the input paths are very complex. It is also known that the optimum placement of the reference signal sensors is a very difficult task.

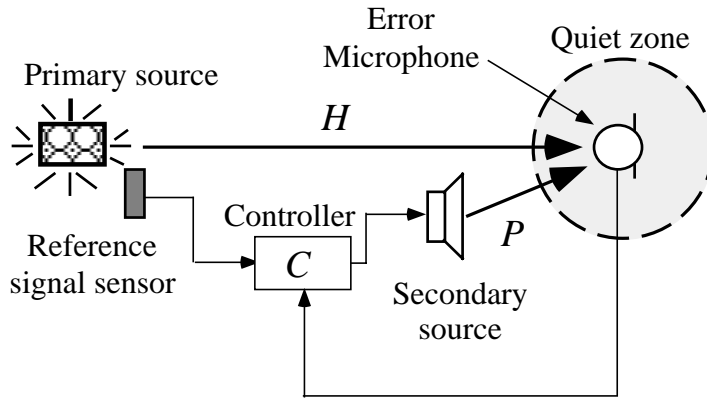


Fig. 1. Configuration of an SISOSE FF-ANC system.

In order to solve these problems, this study focuses on the feedback (FB) ANC system shown in Fig.2. A typical FB-ANC system is based on the tight-coupled monopole (TCM) method⁽⁷⁾, in which error sensors (i.e. microphones) are placed near the control noise sources (i.e. speakers). However, it seems that little research has been reported on the

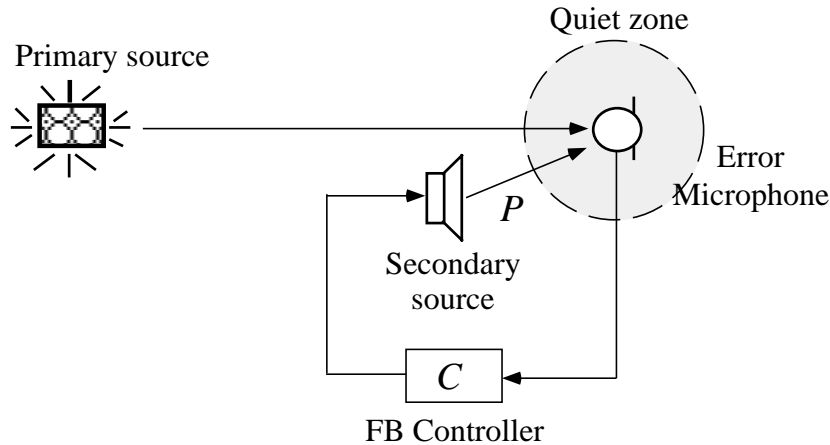


Fig. 2. Configuration of an SISOSE FB-ANC system.

FB-ANC system from the point of view of feedback control engineering. In recent years, some studies based on the feedback control theory have been attempted⁽⁸⁾⁽⁹⁾, although FB-ANC research is still less extensive than FF-ANC research.

The main advantage of the FB-ANC system is its relatively simple configuration because it need no reference signal sensors (see Fig.2). On the other hand, the drawback of FB-ANC is that its noise reduction performance is usually inferior to that of FF-ANC. Therefore, clarifying the performance of an FB-ANC system by applying feedback control theory is considered to be an important prerequisite for further advancements in ANC technology.

The objective of this present study is to design a feedback controller (C in Fig.2) by applying \mathcal{H}_∞ control theory⁽¹⁰⁾ based on a low-order infinite impulse response (IIR) model of the plant. The plant in the FB-ANC system, which is denoted by P in Fig.2 is an acoustic transmission system from a loudspeaker (i.e. the actuator) to an error microphone (i.e. the sensor). The control objective of the FB-ANC system is to reduce the noise level in the vicinity of the error microphone over a low-frequency range below 500 Hz, since noise at more than 500 Hz can be attenuated by conventional passive noise control methods.

In Section II of this paper, the acoustic plant, which contains a loudspeaker, sound field and microphone, is devised by using the physical modeling method in cooperation with a system identification result. The loudspeaker and the microphone are modeled by physical insight with equivalent electrical circuits. The sound field is also represented

by the physical modeling method, assuming that the distance from the speaker to the microphone is sufficiently short relative to the wavelength of the sound to be controlled. Since the phase characteristics of the model are very important for designing the feedback controller, these are fitted to the system identification result that is obtained by the well-known LMS algorithm that assumes a high-order finite impulse response (FIR) model. In Section III, a feedback controller is designed to attenuate the noise level in the vicinity of the error microphone by reducing the sensitivity function over the frequency range of interest. \mathcal{H}_∞ control theory is applied to achieve the control objective, because it can formulate the control specifications in terms of the frequency weighting functions in the frequency domain. In Section IV, the effectiveness of the proposed design procedure is demonstrated by tests. Finally, in Section V, the conclusions are presented. Throughout this paper, the terms "speaker" and "microphone" respectively refer to the control sound source and error sensor used in this study.

II. MODELING OF THE ACOUSTIC PLANT

A. Conventional modeling methods

The most commonly used modeling method in ANC studies is system identification⁽¹¹⁾. In particular, the celebrated LMS algorithm for an FIR model is widely employed because it is simple and does not require squaring, averaging or differentiating operations⁽⁴⁾. Moreover, robustness of the LMS algorithm has also been revealed⁽¹²⁾. However, an FIR model with numerous parameters, for example 64 or 256 or more, is required to precisely describe the plant dynamics. Furthermore, it is not necessarily an FIR model, but a low-order IIR model that is used to design a feedback controller by \mathcal{H}_∞ control theory.

The simplified hyperstable adaptive recursive filter (SHARF) algorithm⁽¹³⁾ has been applied as an IIR modeling method for ANC systems to reduce the parameters in the model. The actual number of parameters, however, was determined by trial and error. As a means of determining the number of parameters with quantitative indicators, an IIR model identification method employing a subspace method has been proposed⁽¹⁴⁾.

Nevertheless, it is not clear to what extent the number of parameters can be reduced while still maintaining the required precision, determining this not only simplifies the

design of the FB controller, but is also an important factor in achieving low-cost ANC. Moreover, a discrete-time model was obtained by the system identification methods just referred, although a continuous-time model is usually more suitable for controller design. For this purpose, the present study employs physical modeling to obtain a reasonable-precision, low-order and continuous-time model to design the feedback control system.

B. Modeling procedure

The proposed modeling procedure for the acoustic plant is summarized as follows.

Step 1 Physical modeling

Step 2 System identification experiment

Step 3 Modeling of implementation devices

Step 4 Parameter tuning

Step 5 Evaluation of model uncertainty

Step 1 Physical modeling

The acoustic plant is composed of three parts: a loudspeaker, an acoustic field, and a microphone. Physical models of these components are derived in the next steps.

Step 1.1 Physical model for the loudspeaker

The loudspeaker, which is considered as a mechanical system, is converted to an equivalent electrical circuit. Transfer function $P_1(s)$ from applied voltage e_0 [V] to vibration velocity v_0 [m/s] of the diaphragm can be described by the following second-order system:

$$P_1(s) = \frac{As}{a_2s^2 + a_1s + a_0} \quad (1)$$

where

$$\begin{aligned} a_2 &= \frac{8}{3}a^3\rho r + mr + Lr_M, \\ a_1 &= r \cdot r_M + C_M L + A^2, \\ a_0 &= C_M r \end{aligned}$$

and ρ [kg/m³] is the air density, a [m] is the cone radius, m [kg] is the diaphragm and coil mass, A is the electrodynamic converter's force factor, r [W] is the coil resistance, L [H] is the coil inductance, r_M [Ns/m] is the mechanical resistance, and C_M [N/m] is stiffness of the diaphragm support.

Step 1.2 Physical model for the sound field

It is assumed in this study that the distance from the speaker to the microphone is sufficiently short relative to the wavelength of the sound to be controlled. Since the effect of direct sounds rather than reflected sounds is predominant even in an enclosed space such as an indoor chamber, the effect of the natural acoustic mode is considered to be minimal. Therefore, a free sound field is assumed for the sake of simplicity.

It is also assumed that the radiative surface of the loudspeaker can be approximated by a planar piston, because the vibration velocity of the diaphragm is equivalent to that of air particles on the diaphragm. Transfer function $P_2(s)$ from diaphragm air particle velocity v_0 [m/s] to the sound pressure at a point on the central axis located distance l [m] from the planar piston can be written by

$$\bar{P}_2(s) = \rho c \left\{ \exp\left(-\frac{l}{c}s\right) - \exp\left(-\frac{\sqrt{l^2 + a^2}}{c}s\right) \right\} \quad (2)$$

where c [m/s] is the speed of sound. If the distance to the measurement point is extremely large relative to the speaker radius, or if the sound contains only low-frequency components, Eq.(2) can be approximated by

$$P_2(s) = \rho \frac{a^2}{2l} s \cdot \exp\left(-\frac{l}{c}s\right). \quad (3)$$

Equation (3) shows that the sound radiation characteristics consist of derivative element $(\rho a^2/2l)s$ and time delay element $\exp\{-(l/c)s\}$. This is a reasonable result since the loudspeaker has a radiative property and the acoustic transmission system is a dead-time type. To examine the approximation accuracy of Eq.(3), the sound pressure levels as a function of distance l are plotted in Fig.3 for sound frequencies of 40 Hz and 500 Hz, respectively. The reason why these frequencies were selected is that the target frequency range of the noise reduction considered in this study is from 40 Hz to 500 Hz. The radius of the cone was $a = 0.0475$ m which is the same as that of the actual speaker used in the experiments which will be described later. From Fig.3, it is clear that Eq.(3) is fully capable of expressing the transfer function of a sound field when the distance is larger than 0.1 m which is shaded in the figures.

Step 1.3 Physical model for the microphone

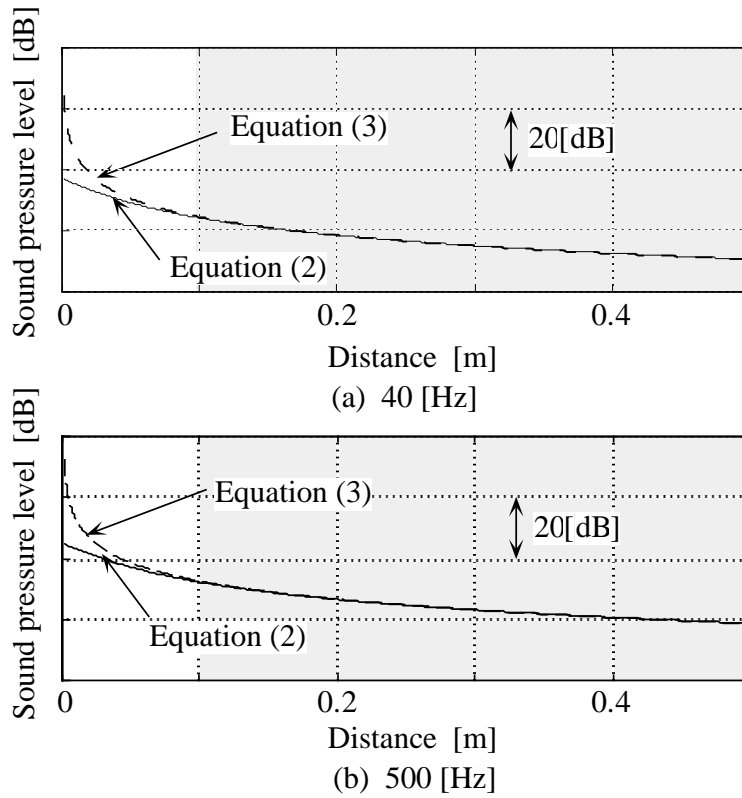


Fig. 3. Relationship between the distance and sound pressure level for 40 Hz (top) and 500 Hz (bottom).

A condenser microphone based on a stiffness control is used as the error sensor in this study. Transfer function of microphone $P_3(s)$ can be written by the proportional gain:

$$P_3(s) = 1, \quad (4)$$

because its frequency response function has flat gain and no phase delay over the frequency range of interest.

Step 1.4 Physical model for the acoustic plant

The physical model for the acoustic plant made up from the three elements, $P_1(s)$, $P_2(s)$ and $P_3(s)$, can be described by

$$\begin{aligned} P_a(s) &= P_1(s)P_2(s)P_3(s) \\ &= \frac{(\rho A a^2 / 2l) s^2}{a_2 s^2 + a_1 s + a_0} \cdot \exp\left(-\frac{l}{c} s\right) \\ &= P_c(s) \exp(-\tau s) \end{aligned} \quad (5)$$

TABLE I
PARAMETERS OF THE LOUDSPEAKER (PANASONIC WS-A10-K).

Parameter	Value
Mass (m)	3.1×10^{-3} kg
Mechanical resistance (r_m)	2.6 Ns/m
Mechanical stiffness (C_m)	1,351 N/m
Coil resistance (r)	2.6 Ω
Coil inductance (L)	5.4×10^{-5} H
Radius of cone (a)	0.0475 m
Force factor (A)	2.98 Tm, N/A
Density of air (ρ)	1.21 kg/m ³
Speed of wave (c)	340 m/s

Substituting the values for the physical parameters of the loudspeaker which is used for the experiments summarized in Table I, $P_c(s)$ and τ for $l = 0.2$ m can be written as

$$P_c(s) = \frac{1.02 \times 10^{-2} s^2}{9.03 \times 10^{-3} s^2 + 12.43s + 3512.6},$$

$$\tau = 5.88 \times 10^{-4}.$$

Therefore, the acoustic plant (5) consists of second-order lumped-parameter system $P_c(s)$ and a distributed-parameter system with time delay element $\exp(-\tau s)$.

Step 2 System identification experiment

In order to refine the physical model (5), a system identification experiment on the acoustic plant was carried out. The experiment was set up as shown in Fig.4.

A pseudo-random signal whose power spectral density is flat below 1 kHz was applied as the identification input signal. The input and output data were measured at a sampling rate of 11,025 Hz, the number of data being 160,000. The sampling rate of the data was reduced by a factor of 8 to 1,378 Hz, this decimation processing being applied in order to focus the identification frequency range below 500 Hz. This correspondingly reduced the number of data for system identification to 20,000. The decimated input and output

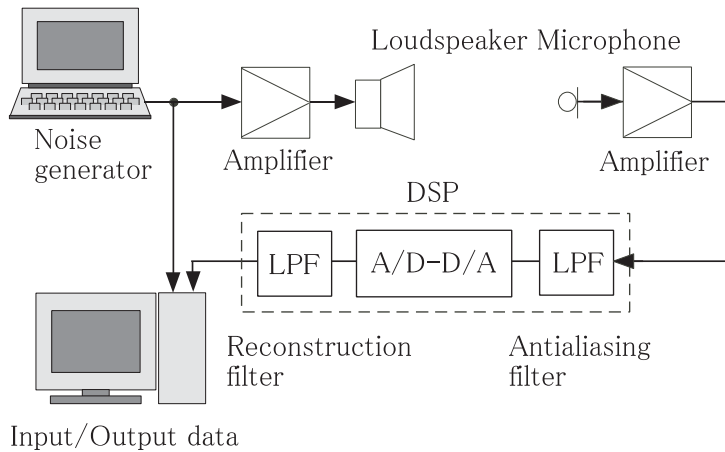


Fig. 4. Set up of the system identification experiment.

signals are shown in Fig.5.

A 64th-order FIR model was used for system identification, and the LMS algorithm was applied to the data. Bode plots of the identification result for $l = 0.2$ m are shown in Fig.6, in which it can be seen that the gain plot of the physical model (dashed line) is almost the same as the system identification result (solid line). However, the phase plot of the physical model differs greatly from the system identification result, because the physical model did not take the DSP dynamics of the implementation device into consideration. This is therefore modeled in the next step.

Step 3 Modeling of the implementation device

The DSP dynamics can be approximated by an all-pass filter:

$$P_i(s) \approx \frac{-0.0008s + 1}{0.0008s + 1} \quad (6)$$

in frequency range below 500 Hz for the Active-5 DSP (Redec Co.) device that was used.

Step 4 Parameter tuning

The plant model can be written for Steps 1 to 3 as follows:

$$\begin{aligned} \bar{P}(s) &= P_a(s)P_i(s) \\ &= \frac{1.02 \times 10^{-2}s^2}{9.03 \times 10^{-3}s^2 + 12.43s + 3512.6} \cdot \frac{-0.0008s + 1}{0.0008s + 1} \cdot \exp(-5.88 \times 10^{-4}s). \end{aligned} \quad (7)$$

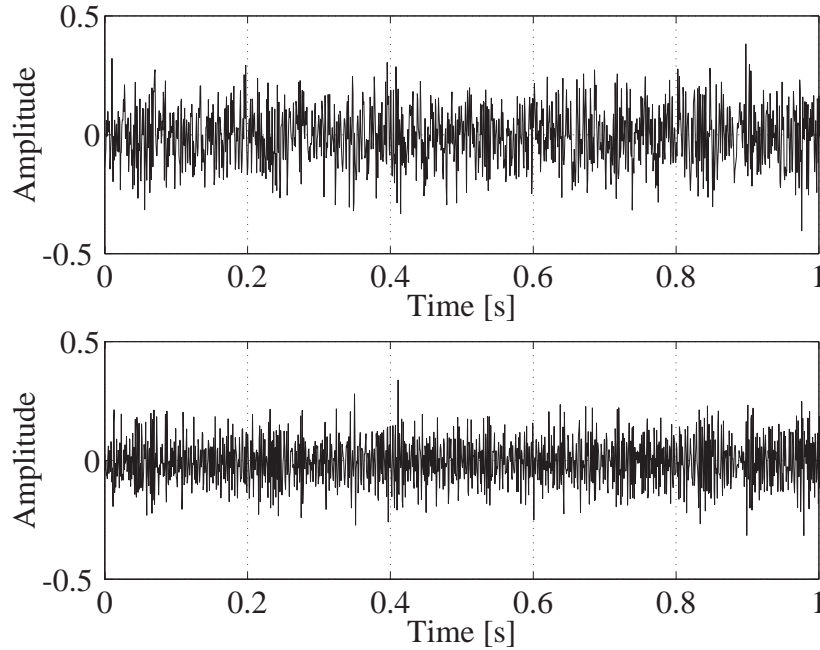


Fig. 5. Input (bottom) and output (top) signals after decimation processing of the original data measured in the system identification experiment.

In general, it is preferable to describe the model by a rational transfer function when the feedback controller has been designed based on robust control theory. In order to approximate $\exp(-5.88 \times 10^{-4}s)$ by a rational function, Pade approximation of order 2:

$$P_d(s) = \frac{1 - \alpha s + (\alpha s)^2/12}{1 + \alpha s + (\alpha s)^2/12} \quad (8)$$

is applied. Parameter α is tuned so that the phase characteristics of

$$P_{nom}(s) = P_a(s)P_i(s)P_d(s)$$

match the system identification result obtained in Step 2 over the frequency range of 40 ~ 500 Hz, where $P_{nom}(s)$ denotes a nominal model of the plant. $\alpha = 0.0035$ was obtained by trial and error.

As a result, the plant can be described by a 5th-order IIR model represented by

$$\begin{aligned} P_{nom}(s) &= P_p(s)P_d(s)P_f(s) \\ &= \frac{0.0203s^2}{0.00903s^2 + 12.43s + 3512.6} \cdot \frac{-0.0008s + 1}{0.0008s + 1} \cdot \frac{1.02 \times 10^{-6}s^2 - 1.75 \times 10^{-3}s + 1}{1.02 \times 10^{-6}s^2 + 1.75 \times 10^{-3}s + 1} \end{aligned} \quad (9)$$

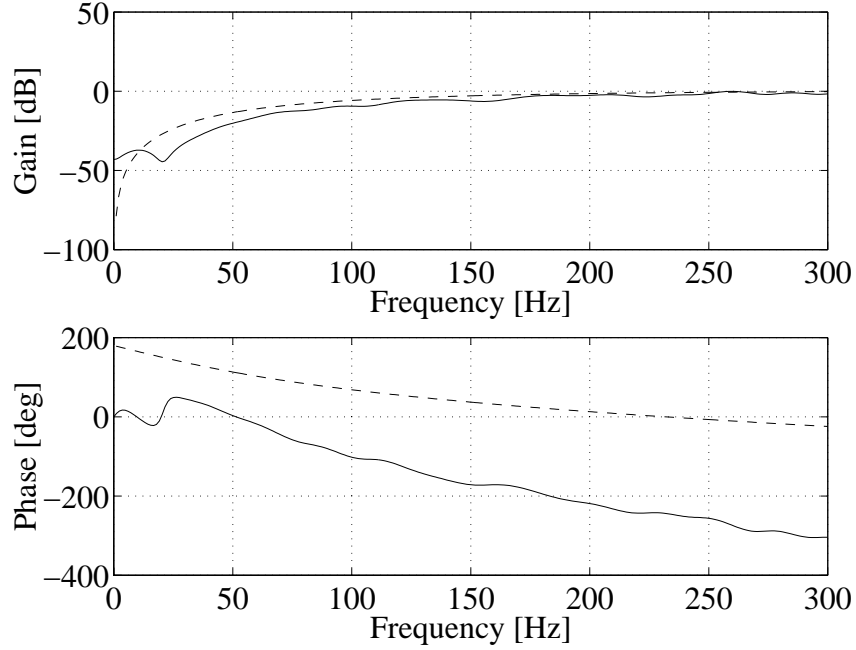


Fig. 6. Comparison between the system identification result (solid line) and physical model (dashed line) for $l = 0.2$ m.

A Bode plot of the model is shown by the solid line in Fig. 7, in which the dashed line shows the system identification result based on the 64th-order FIR model. It is clear that the 5th-order IIR model matches well with the conventional 64th-order FIR model over the frequency range of 40 ~ 500 Hz. Since the proposed approach is based on physical modeling, a continuous-time model can be directly obtained, which is very suitable for feedback controller design.

Step 5 Evaluation of the model uncertainty

An evaluation of the model uncertainty is required to design an FB-ANC system by \mathcal{H}_∞ control theory. The additive uncertainty can be evaluated by

$$\Delta_a(j\omega) = P_{id}(j\omega) - P_{nom}(j\omega) \quad (10)$$

where $P_{id}(j\omega)$ is a precise model which was obtained by system identification in Step 2 and $P_{nom}(j\omega)$ is the nominal model which was calculated in Step 4.

In order to cover the additive model uncertainty $|\Delta_a(j\omega)|$, a frequency weighting function

$$W_T(s) = \frac{2.9(s + 62.8)}{s + 5027} \quad (11)$$

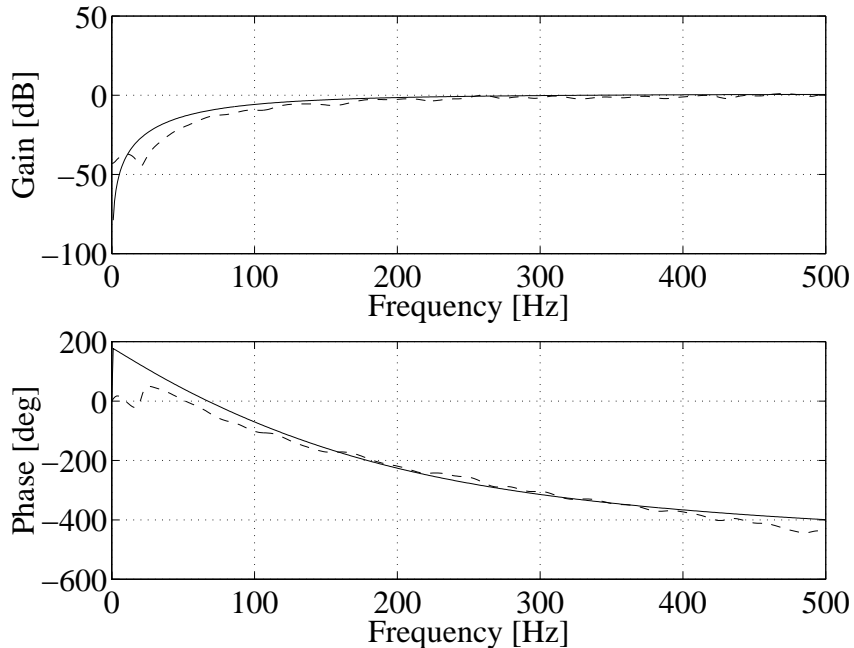


Fig. 7. Proposed model result (solid line) and system identification result (dashed line) for $l = 0.2$ m.

was chosen for $l = 0.2$ m. Since the order of $W_T(s)$ influences the order of the designed controller, a 1st-order high-pass filter was employed. Fig.8 shows $|\Delta_a(j\omega)|$ (dashed line) and $|W_T(j\omega)|$ (solid line). $W_T(s)$ plays an important role in robust stabilization.

III. FEEDBACK CONTROLLER DESIGN INCORPORATING \mathcal{H}_∞ CONTROL

The design of feedback controller $C(s)$ in Fig.2 is based on the nominal model described by Eq.(9) and frequency weighting function $W_T(s)$ for the additive model uncertainty.

The control specifications of the FB-ANC system are as follows:

S1: Stabilization of the closed-loop system

S2: Attenuation of the sensitivity function in the low-frequency range, especially around 150 Hz

S3: Robust stabilization against the additive model uncertainty.

In S2, sensitivity function $S(s)$, which is the transfer function from noise d to error e , is defined by

$$S(s) = \frac{1}{1 + P(s)C(s)}. \quad (12)$$

Also, we aim at attenuating noise level at 150 Hz, because low frequency road noise below

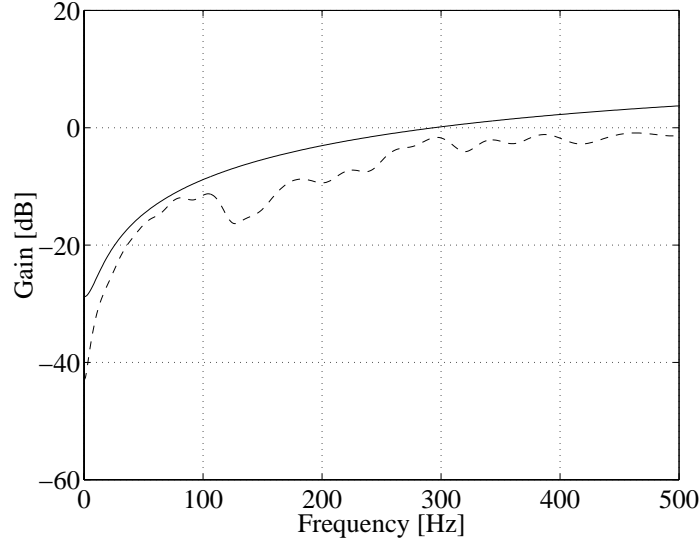


Fig. 8. Additive model uncertainty $|\Delta_a(j\omega)|$ (dashed line) and corresponding frequency weighting function $|W_T(j\omega)|$ (solid line) for $l = 0.2$ m.

200 Hz is difficult to reduce by passive methods without increasing car weight in an actual car development.

\mathcal{H}_∞ control was adopted for the feedback controller design method, because it can assign the appropriate attenuation performance according to the sensitivity function. The nominal performance can be described by

$$\|W_S(s)S(s)\|_\infty < 1 \quad (13)$$

where $W_S(s)$ is a frequency weighting function. To meet the control specification S2,

$$W_S(s) = \frac{Ks^2}{s^2 + 2\zeta\omega_n s + \omega_n^2} \quad (14)$$

was applied where $\omega_n = 2\pi \times 150$. The other parameters K and ζ were tuned by trial and error based on the shape of $|S(j\omega)|$ so as to attenuate the noise level at 150 Hz. In this experiment, $K = 0.6$ and $\zeta = 1/14$ were selected.

The design specification S3 is described by

$$\|W_T(s)T(s)\|_\infty < 1 \quad (15)$$

where $T(s)$ is the complementary sensitivity function defined by

$$T(s) = \frac{P(s)C(s)}{1 + P(s)C(s)} \quad (16)$$

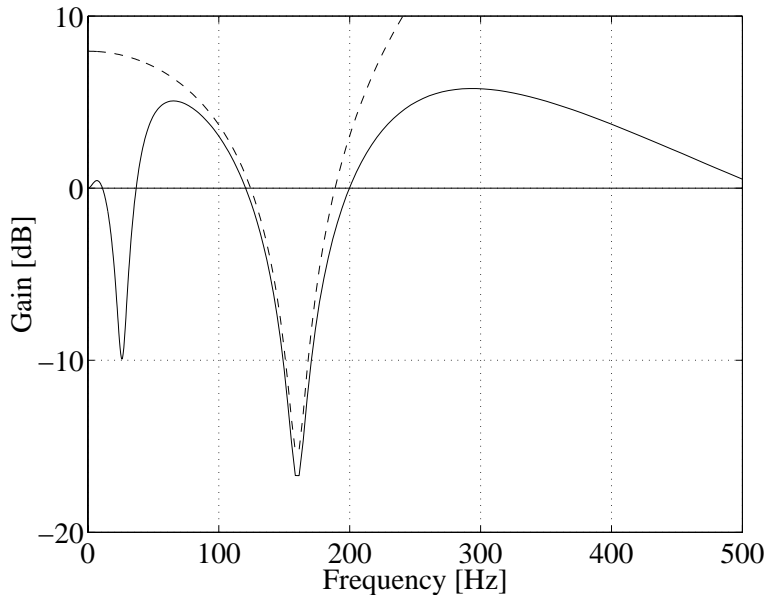


Fig. 9. Sensitivity function $|S(j\omega)|$ (solid line) and frequency weighting function $|W_S(j\omega)|^{-1}$ (dashed line).

which is the transfer function from noise d to the plant output. Frequency weighting function $W_T(s)$ is given by Eq.(11) in the previous section. The control problem considered here is known as a mixed sensitivity type.

The \mathcal{H}_∞ controller was designed in continuous-time by the Glover and Doyle method⁽¹⁵⁾. The resulting sensitivity function is shown in Fig. 9, indicating a noise attenuation by the feedback controller of about 15 dB at a frequency of 150 Hz. It can be seen from Fig. 9 that there are amplification areas such as 40 ~ 120 Hz and 200 ~ 500 Hz, where the sensitivity function is greater than 0 dB. This is an inherent drawback of the FB-ANC system, which is known as the water-bed effect, because the acoustic plant is a non-minimum phase system due to the time delay⁽¹⁶⁾. In this study, however, we aim at attenuating the noise in a particular frequency band, which is around 150 Hz in our specifications, at the cost of amplification areas existing.

The obtained continuous-time controller can be digitized by bilinear transformation as follows:

$$s = 2f_s \frac{1 - z^{-1}}{1 + z^{-1}}.$$

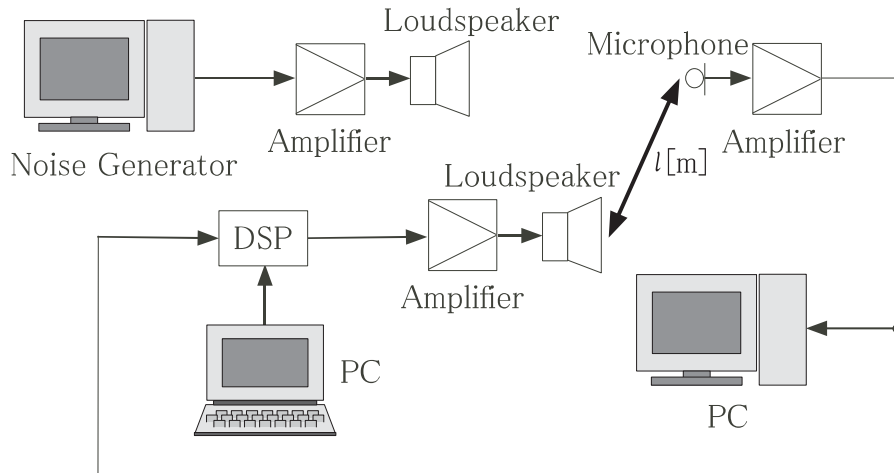


Fig. 10. Configuration of the experimental apparatus.

The discrete-time controller,

$$C(z) = \frac{b_0 + b_1 z^{-1} + \dots + b_8 z^{-8}}{1 + a_1 z^{-1} + \dots + a_8 z^{-8}}$$

can then be obtained in which the sampling rate is $f_s = 3$ kHz. The values for these coefficients are $a_1 = -5.315$, $a_2 = 12.24$, $a_3 = -16.17$, $a_4 = 13.74$, $a_5 = -7.915$, $a_6 = 3.024$, $a_7 = -0.6469$, $a_8 = 0.04360$, $b_0 = 0.3173$, $b_1 = -1.575$, $b_2 = 2.635$, $b_3 = -1.138$, $b_4 = -1.685$, $b_5 = 2.445$, $b_6 = -1.252$, $b_7 = 0.2680$, and $b_8 = -0.01548$.

IV. EXPERIMENTS

The performance of the proposed feedback controller was tested by the experimental apparatus shown in Fig.10. Pseudo road noise was used to simulate the noise inside an automobile.

The plot of the A-weighted relative sound pressure level for $l = 0.2$ m is shown in Fig. 11. It is clear that the FB-ANC system attenuates the noise level at 150 Hz by about 15 dB, this being the predicted attenuation level based on the sensitivity function.

It is known that the zone of quiet, within which the pressure is at least 10 dB below that due to the primary source, is a sphere with a diameter of about one-tenth of a wavelength⁽¹⁾. Therefore, the zone of quiet in this experiment is expected to be a sphere with a diameter of 0.226 m, since the frequency of the target noise is 150 Hz.

By a similar modeling and controller design procedure, an FB-ANC system for $l = 0.5$ m was designed, whose design specifications are the same as those for $l = 0.2$ m. A Bode plot of the obtained model is shown in Fig.12. It is clear that the proposed modeling procedure is capable of being applied to the acoustic plant with $l = 0.5$ m.

The experimental result is shown in Fig.13. It can be seen that the designed system attenuates the noise level at 150 Hz by about 11 dB and that the noise attenuation performance is degraded as distance l becomes longer. The experimental results concur with those of the theoretical study on FB-ANC systems⁽¹⁶⁾.

An acoustic plant with $l = 1$ m was also modeled, the result being shown in Fig.14, where the dashed line represents the system identification result. It is clear from the dashed line that the natural acoustic modes are dominant in this acoustic plant, so the proposed modeling procedure could not be applied. Instead of this method, the curve fitting method in the frequency domain was applied such that the gain and phase characteristics below 200 Hz match the system identification result.

The experimental result is shown in Fig.15. It is surprising that the designed system attenuates the noise level at 150 Hz by about 10 dB. However, the attenuation zone, i.e. the difference between the dashed line and solid one, has shrunk in comparison with the cases for $l = 0.2$ and 0.5 m.

V. CONCLUSIONS

The modeling and controller design procedure for an FB-ANC system for free sound fields is proposed. The acoustic plant was modeled as a low-order IIR model by the physical modeling method in conjunction with the system identification result under the assumption that the distance was sufficiently short relative to the wavelength of the sound to be controlled. A feedback controller was next designed to attenuate the noise level in the vicinity of the error sensor by \mathcal{H}_∞ control theory based on the IIR model. Finally, the effectiveness of the proposed design procedure was demonstrated by experimental tests.

A free sound field has been assumed in this study. A systematic modeling and controller design procedure for an acoustic field with reverberation will be the subject of further study.

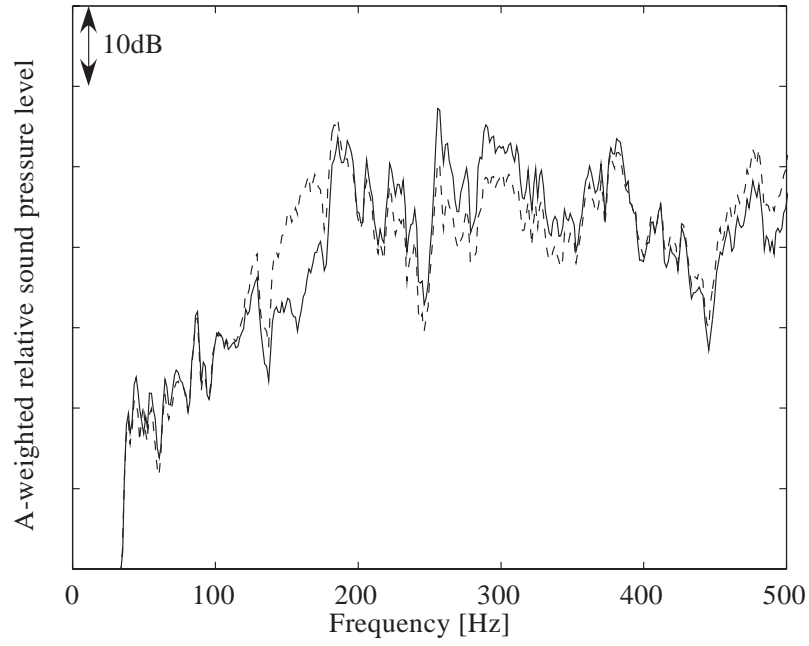
ACKNOWLEDGMENTS

The authors thank Mr. M.Ogawa, Mr. T.Sannoudou, Mr. M.Hirano, and Miss Y.Yoneya of Utsunomiya University and Mr. A.Takahashi of Honda R & D Center for their help in the numerical simulations and experiments.

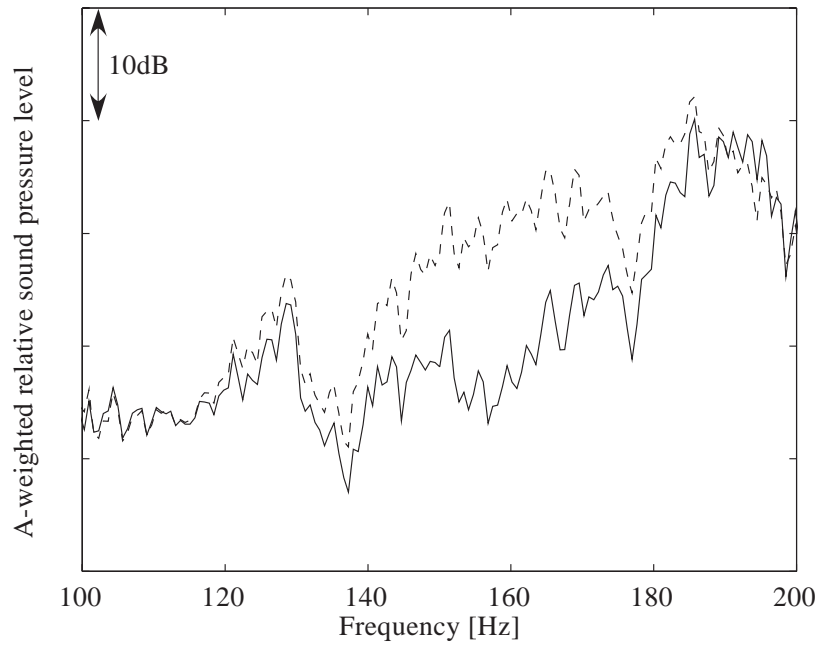
References

- (1) Nelson,P.A. and Elliott,S.J., *Active control of sound*, Academic Press (1993).
- (2) Kuo,S.M. and Morgan,D.R., *Active noise control systems – Algorithms and DSP implementations*, John Wiley & Sons (1996).
- (3) Sano,H., Adachi,S. and Kasuya,H., Application of a Least Squares Lattice Algorithm to Active Noise Control for an Automobile, Trans. ASME, J. of Dynamic Systems, Measurement, and Control, Vol. 119, No. 2 (1997), p. 318–320.
- (4) Widrow,B. and Sterns,S.D., *Adaptive Signal Processing*,Prentice-Hall (1985).
- (5) Bernhard,R.J., Road Noise Inside Automobiles, Proc. Active95 (1995), p. 21–32.
- (6) Sutton,T.J., Elliott,S.J. and McDonald,A.M., Active Control of Road Noise Inside Vehicles, Noise Contr. Eng. J., Vol. 42, No. 4 (1994), p. 137–147.
- (7) Eghtesadi,K., Hong,W.K.W. and Leventhall,H.G., The Tight-Coupled Monopole Active Attenuator in a Duct, Noise Contr. Eng. J., Vol. 20, No. 1 (1983), p. 16–20.
- (8) James,J., Akers,J., Venugopal.R., Lee,R., Sparks,A., Washabaugh, P. and Berstein,D., Modeling, Identification, and Feedback Control of Noise in an Acoustic Duct, IEEE Trans. Control Systems Technology, Vol. 4, No. 3 (1996), p. 283–291.
- (9) Adachi,S. and Sano,H., Application of Two-Degree-Of-Freedom Type Active Noise Control Using IMC to Road Noise Inside Automobiles, Proc. of 35th IEEE Conf. Decision and Contr. (1996), p. 2794–2795.
- (10) Doyle,J.C., Francis,B.A. and Tannenbaum,A.R., *Feedback Control Theory*, Macmillan (1992).
- (11) Ljung,L., *System Identification – Theory for the User (2nd ed.)*, Prentice Hall PTR (1999).
- (12) Hassibi,B.,Sayed, A.H. and Kailath,T., Optimality of the LMS Algorithm, IEEE Trans. on Signal Processing, SP-44-2 (1997), p. 267–280.
- (13) Kuo,S.M. and Tappia,J., The Implementation of Modified Leaky SHARF Algorithm for the Active Noise Cancellation, Proc. IEEE ASSP Workshop Applications of Signal Processing to Audio and Acoustics (1989).
- (14) Sano,H. and Adachi,S., Two-Degree-Of-Freedom Active Control of Road Noise Inside Automobiles, Proc. Active97, (1997), p. 543–546.

- (15) Glover, K. and Doyle, J.C., State-Space Formulae for All Stabilizing Controller that Satisfy an \mathcal{H}_∞ -Norm Bound and Relations to Risk Sensitivity, *Systems & Control Letters*, Vol.11 (1988), p. 167–172.
- (16) Sano, H., Miyamoto, S, and Adachi, S., Two-Degree-Of-Freedom Active Noise Control with Internal Model Control in Feedback Control, *Trans. of the Japan Society of Mechanical Engineers*, (in Japanese), Vol. 63 , No. 608 (1997), p. 1208-1213.



(a) Frequency range of 0 ~ 500 Hz.



(b) Frequency range of 100 ~ 200 Hz.

Fig. 11. Sound pressure level of the FB-ANC system (solid line), where the dashed line indicates the original sound pressure level for $l = 0.2$ m.

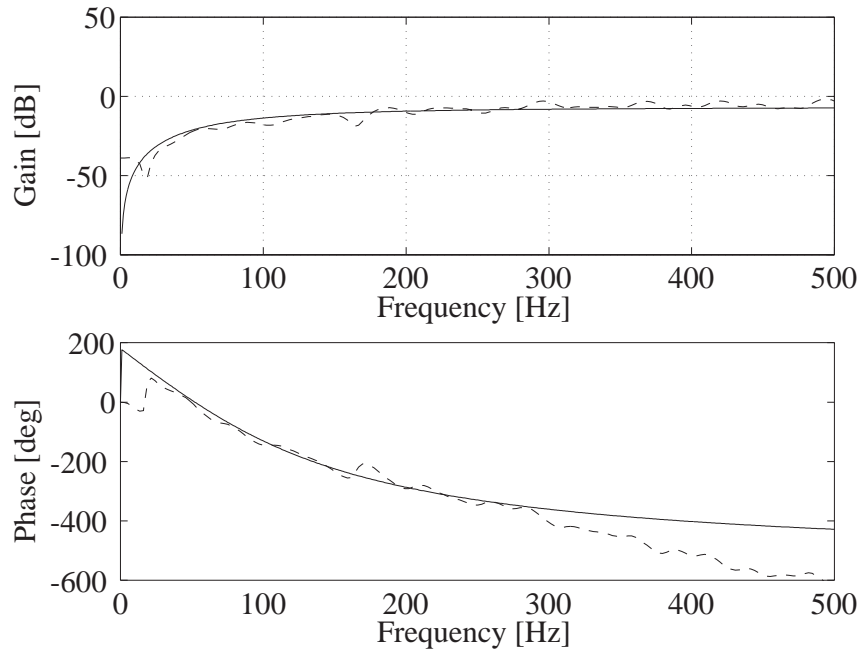


Fig. 12. Proposed modeling result (solid line) and system identification result (dashed line) for $l = 0.5$ m.

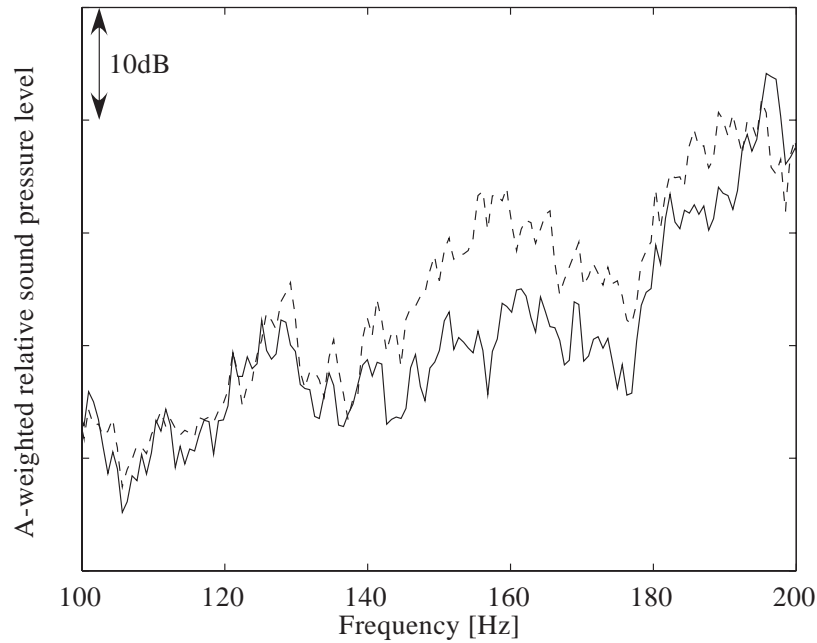


Fig. 13. Sound pressure level of the FB-ANC system (solid line), where the dashed line indicates the original sound pressure level for $l = 0.5$ m.

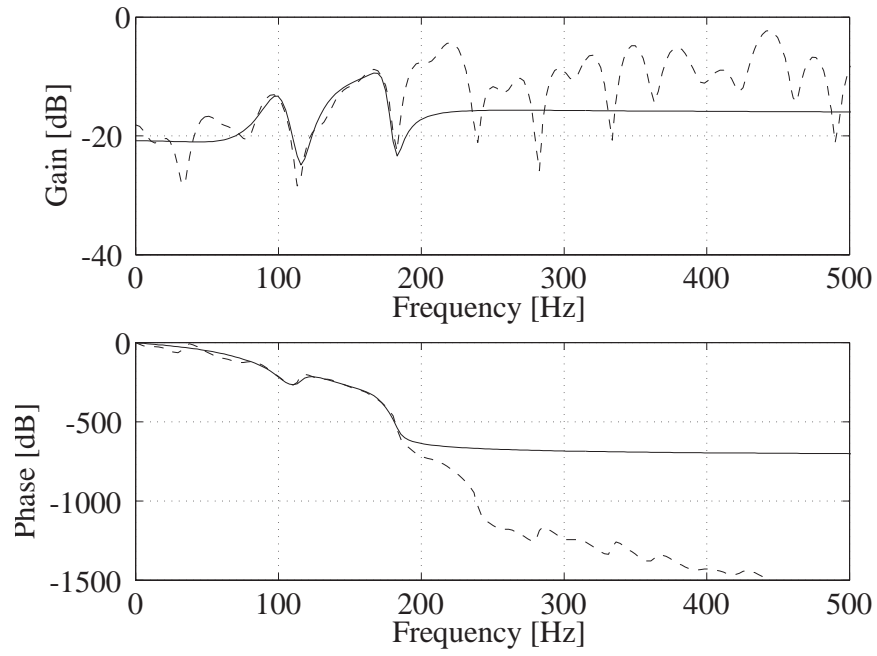


Fig. 14. Modeling result by curve fitting (solid line) and the system identification result (dashed line) for $l = 1$ m.

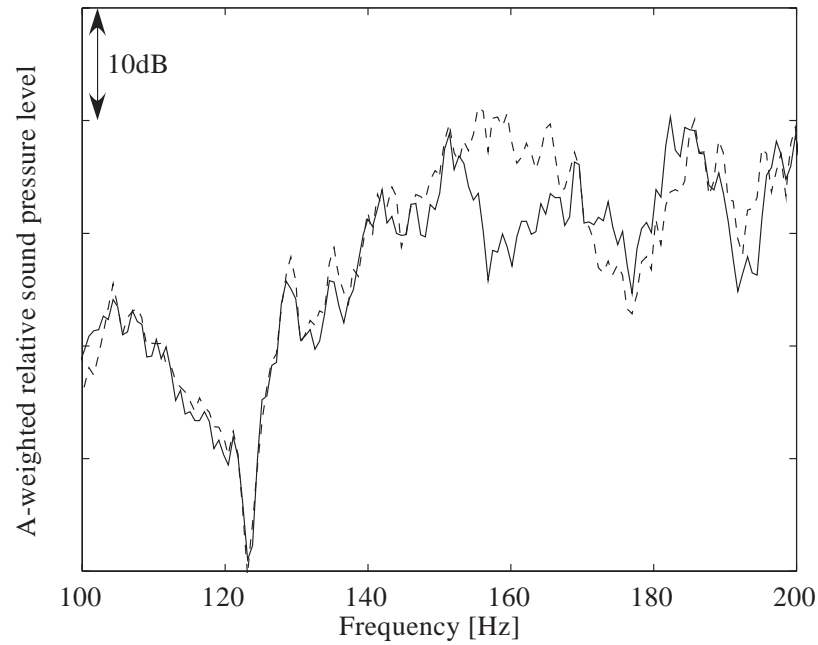


Fig. 15. Sound pressure level of the FB-ANC system (solid line), where the dashed line indicates the original sound pressure level for $l = 1$ m.